nature astronomy

SUPPLEMENTARY INFORMATION
https://doi.org/10.1038/s41550-018-0687-6

In the format provided by the authors and unedited.

The case for seasonal surface changes at Titan's lake district

Shannon M. MacKenzie[1,2*], Jason W. Barnes[2], Jason D. Hofgartner[3], Samuel P. D. Birch[4], Matthew M. Hedman[2], Antoine Lucas[5], Sebastien Rodriguez[5], Elizabeth P. Turtle[1] and Christophe Sotin[3]

[1]Applied Physics Laboratory, John Hopkins University, Laurel, MD, USA. [2]Department of Physics, University of Idaho, Moscow, ID, USA. [3]Jet Propulsion Laboratory/California Institute of Technology, Pasadena, CA, USA. [4]Department of Astronomy, Cornell University, Ithaca, NY, USA. [5]Institut de Physique du Globe de Paris, Sorbonne Paris Cité, Univ Paris Diderot, CNRS, Paris, France. *e-mail: shannon.mackenzie@jhuapl.edu

nature astronomy

SUPPLEMENTARY INFORMATION

https://doi.org/10.1038/s41550-018-0687-6

In the format provided by the authors and unedited.

The case for seasonal surface changes at Titan's lake district

Shannon M. MacKenzie[1,2*], Jason W. Barnes[2], Jason D. Hofgartner[3], Samuel P. D. Birch[4], Matthew M. Hedman[2], Antoine Lucas[5], Sebastien Rodriguez[6], Elizabeth P. Turtle[1] and Christophe Sotin[3]

[1]Applied Physics Laboratory, John Hopkins University, Laurel, MD, USA. [2]Department of Physics, University of Idaho, Moscow, ID, USA. [3]Jet Propulsion Laboratory/California Institute of Technology, Pasadena, CA, USA. [4]Department of Astronomy, Cornell University, Ithaca, NY, USA. [5]AIM CEA-Saclay, Université Paris Diderot, USPC, Paris, France. [6]Institut de Physique du Globe de Paris (IPGP) Université Paris Diderot, Paris, France.
*e-mail: shannon.mackenzie@jhuapl.edu

The case for seasonal surface changes at Titan's lake district
Supplementary Information

In Supplemental Figure 1 we show an empty lake and a filled lake, each illuminated by the RADAR signal (solid black line). The return signal from the empty lake (red) is a combination of a quasi-specular component (σ_G^0) and a diffuse component (σ_d^0). Hayes et al. (2011) found that a Gaussian expression for the quasi-specular component provided a better fit to the observed σ^0 of empty lakes observed by RADAR. Their result is plotted in Figure 3 as the solid red line with the 95% confidence interval represented by red shading.

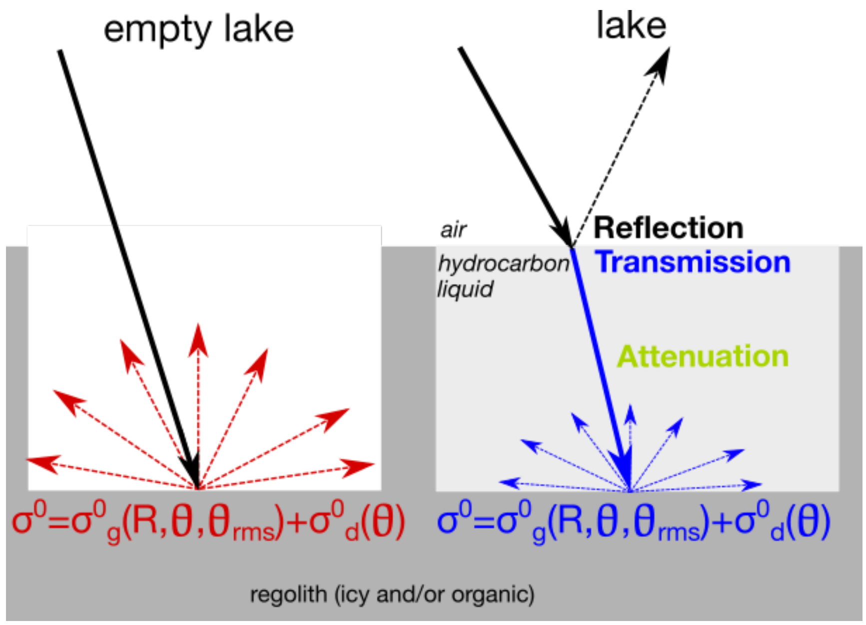

Supplemental Figure 1: Radar scattering off empty lake bottoms (left) and filled lakes (right). Colors correspond to cases plotted in Figure 3 and in Supplemental Figure 2. Backscattering off the solid bottom in both cases is a function of both quasi-specular scattering (σ_g; a function of the Fresnel reflection coefficient R, the incidence angle θ, and the surface tilt angle θ_{rms}) and diffuse scattering (σ_d). (Arrow length does not convey energy magnitude.)

Signal returned from the filled lake case, however, has a different scattering history, summarized in the right panel of Supplemental Figure 1. Indeed, Hayes et al. (2011) found that empirically fitting the σ^0 of partially-filled lakes (blue line of Figure 3; shading represents 95% confidence intervals) –including those shown as blue circles in Figure 3–with the sum of a Gaussian quasi-specular scattering function and a volume scattering function required different parameters than for the empty lake basins (red line of Figure 3). In both cases, the free parameters included in the fit include the real dielectric constant, surface tilt angle, and the diffuse signal power.

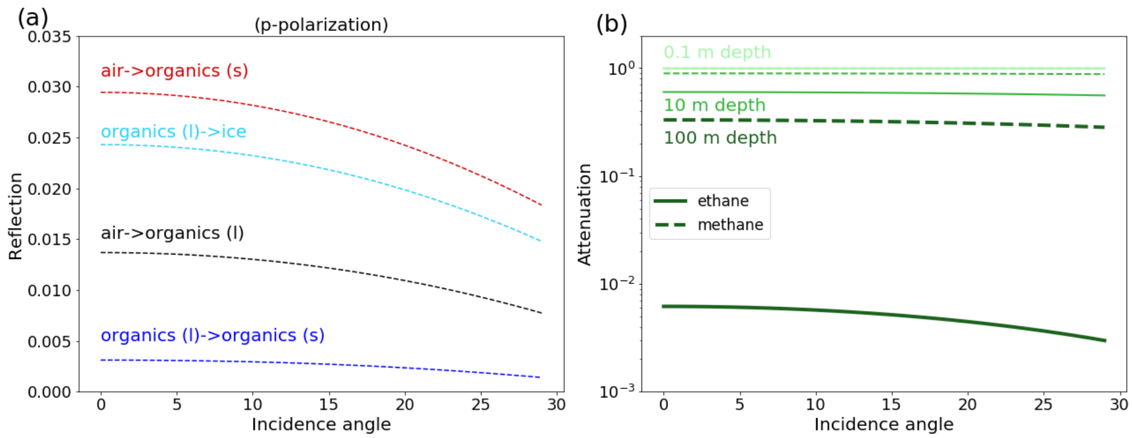

Supplemental Figure 2: Reflection (a) and attenuation (b) coefficients for Titan materials. We plot only the p-polarization case for ease of interpretation. The reflection coefficients are calculated with the Fresnel equations for boundaries between air ($\epsilon \sim 1$), liquid organics ($\epsilon \sim$1.6), solid organics ($\epsilon \sim$2), and water ice ($\epsilon \sim$3). The one-way attenuation coefficient as a function of incidence angle (θ) is calculated via $A = e^{\frac{4\pi\kappa d}{\lambda cos(\theta)}}$ for liquid depths (d) 0.1, 10, and 100 m. λ is 2.17 cm, the *Cassini* RADAR wavelength. κ is the imaginary component of the dielectric constant, as calculated for methane and ethane by Mitchell et al. (2015). Note that at 0.1 m, attenuation is so small that the methane and ethane lines appear superimposed. Most of the power incident on the lakes is transmitted through the liquid column to the lake floor.

Evidence from both Cassini RADAR (Wye et al. 2009, Zebker et al. 2014) and VIMS (Stephan et al. 2010, Barnes et al. 2011) constrains the surface of Titan's lakes as smooth enough that the vertical deviations are much less than a radar wavelength (in the absence of waves). Scattering at the atmosphere-lake boundary can therefore be described by the Fresnel equations. Supplemental Figure 2 shows the reflection and attenuation factors for a variety of scenarios with Titan-relevant materials. If the empty lake floor were as smooth as the liquid, the Supplemental Figure 2a shows that the air-solid organic boundary (red line) allows more reflection than an air-liquid organics boundary (light blue line). In either case, the reflected power

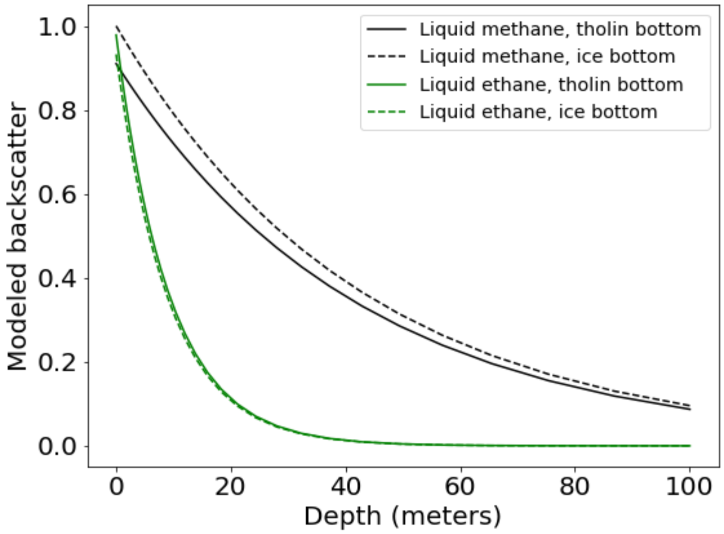

Supplemental Figure 3: Backscatter relative to the brightest modeled backscatter, a 10 cm deep ethane lake with an icy lake floor.

is a small fraction. Of course, the empty lake floors on Titan are not in reality as smooth as the lakes, but this comparison shows the relative effect of dielectric constant contrast: even shallow lakes (where attenuation is minimal) will appear darker than dry, solid surfaces. (The Hayes et al. (2011) empirical fit (Figure 3 red line) shows a realistic description of the quasispecular and diffuse scattering components of an empty-lake floor.)

Within the lakes, the transmitted signal experiences some extinction (absorption plus scattering) traveling through the liquid column before scattering off of (and within) the lake floor. The effective extinction of several liquid bodies on Titan has been measured to be small and consistent with pure methane-ethane-nitrogen mixtures with little to no scattering in the liquid volume (Mastrogiuseppe et al., 2014, 2018a, 2018b; Mitchell et al., 2015). Supplemental Figure 2b demonstrates that for a pure methane or ethane liquid, attenuation via absorption does not significantly affect the brightness for depths of < 10 m. Thus, in the event that the phantom lakes are pools shallow enough to have evaporated and/or infiltrated between RADAR and IR observations, attenuation within the column is not significant. However, as noted in the discussion of the Fresnel reflection coefficient plot, a shallow lake will still appear darker to RADAR than the surrounding surface.

We note, then, that there is a degeneracy in lake-darkening mechanisms (attenuation within the liquid and lakefloor brightness) which in turn have their own degeneracies: composition, depth, scatterers for attenuation and composition, roughness, diffuse component for lake floors. A shallow lake with a dark lake bottom can look as dark as a deeper lake with a bright lake bottom. We show this in Supplemental Figure 3 using a modified 2 layer model from Hayes et al. (2011), the methane and ethane dielectric properties of Mitchell et al. (2015), and ice and solid tholin dielectric properties of Paillou et al. (2008). We assume that backscatter is $\approx T(\theta_{lake})T(\theta_{surface})A(d,\theta_{lake})A(d,\theta_{surface})\sigma_{bed}$ where T is the transmission coefficient at the atmosphere-lake boundary (incident at angle θ_{lake}) and at the lake-surface boundary (incident at angle $\theta_{surface}$). A is the absorption coefficient, as calculated in Supplemental Figure 2, which is a function of incidence angle and liquid depth d. In Supplemental Figure 3 we normalize to the brightest example calculated (methane liquid, ice floor, liquid depth of 10 cm). The backscatter value is not unique to specific different depths if liquid or floor compositions differ between lakes.

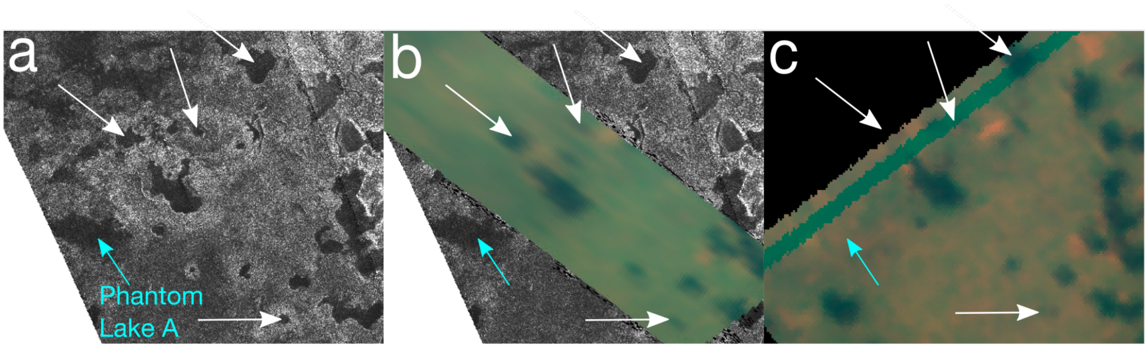

Supplemental Figure 4: Some lakes (white arrows) plotted in Figure 3 have a higher σ^0 than the phantom lakes. Unlike the phantom lakes, these lakes were later observed by VIMS as consistent with the spectral behavior of lakes. (a) Noise-subtracted RADAR swaths T16 and T19 (b) VIMS cube CM_1764551088_1-57 colored according to R= 5 μm, G= 2 μm, and B = 1.3 μm. (c) VIMS cube CM_1764550739_16 colored with the same color scheme.

This degeneracy may explain, for example, how some lakes observed in RADAR swath T16 (indicated by white arrows) appear brighter than the phantom lakes in Figure 3 (and, more generally, the scatter of the lake points in Figure 3). The brighter SAR signal suggests then that these lakes are shallower (less attenuation) or have brighter floors than the phantom lakes. Later observations by VIMS, however, show that these features' spectral characteristics are consistent with being liquid-filled; that is, they appear blue in Supplemental Figure 4. These lakes have therefore not completely emptied. Given their proximity to the phantom lakes, these still-filled lakes likely experience the same rate of evaporation. They can remain filled by (1) being initially deeper than the phantom lakes, (2) having a higher ethane content as it is less volatile on seasonal timescales, or (3) having a less permeable floor that slows or prevents infiltration.

Using the same methods as Brown et al. (2008), we searched for the presence of an ethane absorption feature within the phantom lakes by taking the ratio of the phantom lake's spectra to nearby land pixels to minimize atmospheric effects. In Supplemental Figure 5 we show the results for each phantom lake and a nearby lake.

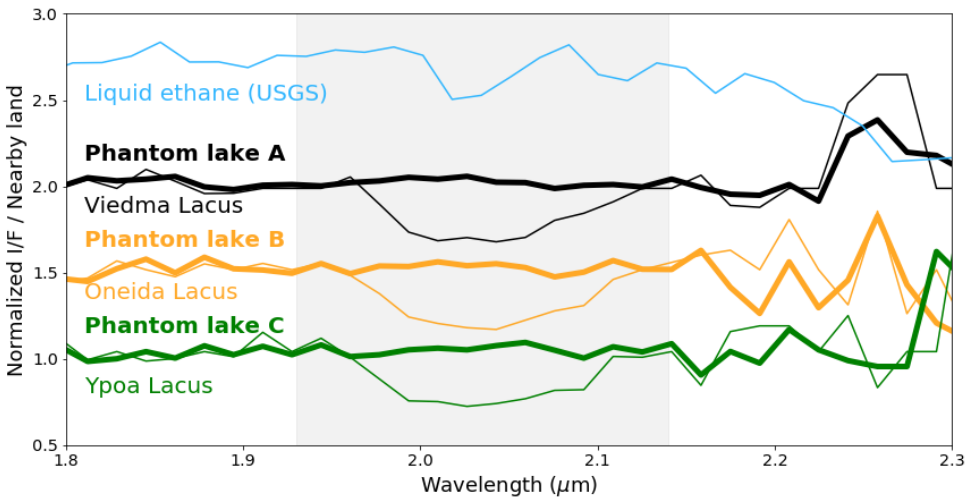

Supplemental Figure 5: Ethane spectra convolved to the VIMS wavelengths (Kokaly et al. 2017) compared to the spectra of phantom lakes and nearby filled lakes, ratioed with nearby land pixels to remove atmospheric effects. While each lake shows a dip in the 2 μm window consistent with the ethane absorption feature described by Brown et al. (2008) identified in Ontario Lacus, the phantom lakes do not. The atmospheric window through which VIMS sees down to the surface is indicated by grey shading.

We can rule out clouds as responsible for the IR-brightness of the phantom lakes because the spectral signature of the phantom lakes does not change over multiple observations by ISS and VIMS and because the spectral behavior of the phantom lakes are inconsistent with clouds. In Supplemental Figure 6 we show the T96 cube that best resolves the phantom lakes (a) and a low-lying cloud over Ligeia Mare (b) observed in T104. In panels (c-d) we show how the slopes in the 2 μm and 2.75 μm window wings differ for cloud features than for surface features due to the absorption of methane. Methane absorption increase away from the window center and thus probe different levels of the atmosphere (e.g. Griffith et al. 2005). Rodriguez et al. (2009, 2011) also documented an increased brightness in the 5 μm window relative to 2 μm window for clouds, which is evident for the cloud over Ligeia but not the phantom lakes (d-e).

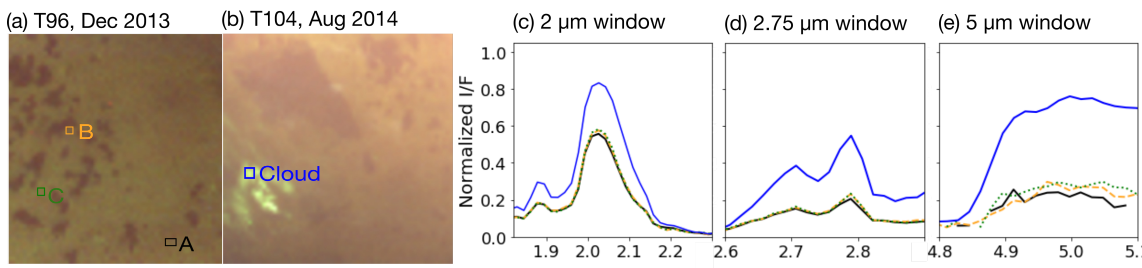

Supplemental Figure 6: VIMS data demonstrating that phantom lakes do not demonstrate cloud-like spectral behavior. Using the color scheme of Barnes et al. (2007) where VIMS channels 66,110, and 107 are assigned to RGB, clouds appear bright green-blue in views of the north pole from T96 (a; CM_1764550739_16) and T104 (b;CM_1787307197_1). Due to the wavelength shift of the VIMS instrument, the exact values of these channels have shifted since the observations of Barnes et al. (2007). Spectra of the cloud (blue) and phantom lakes A, B, and C (black, yellow, green) are plotted in three of the atmospheric windows (c-e) to highlight the difference between atmospheric and surface spectra. The pixels of (a) and (b) used to generate the spectra in (c-e) are indicated with corresponding colored boxes.

References

Barnes, Jason W., et al. "VIMS spectral mapping observations of Titan during the Cassini prime mission." Planetary and Space Science 57.14-15 (2009): 1950-1962.

Barnes, Jason W., et al. "Wave constraints for Titan's Jingpo Lacus and Kraken Mare from VIMS specular reflection lightcurves." Icarus 211.1 (2011): 722-731.

Brown, R. H., et al. "The identification of liquid ethane in Titan's Ontario Lacus." Nature 454.7204 (2008): 607.

Griffith, Caitlin A., et al. "The evolution of Titan's mid-latitude clouds." Science 310.5747 (2005): 474-477.

Hayes, A. G., et al. "Transient surface liquid in Titan's polar regions from Cassini." Icarus 211.1 (2011): 655-671.

Kokaly, Raymond F., et al. "USGS spectral library version 7". No. 1035. US Geological Survey, 2017.

Mastrogiuseppe, M., et al. "Cassini radar observation of Punga Mare and environs: Bathymetry and composition." Earth and Planetary Science Letters 496 (2018): 89-95.

Mastrogiuseppe, Marco, et al. "Bathymetry and composition of Titan's Ontario Lacus derived from Monte Carlo-based waveform inversion of Cassini RADAR altimetry data." Icarus 300 (2018): 203-209.

Mastrogiuseppe, Marco, et al. "Radar Sounding Using the Cassini Altimeter: Waveform Modeling and Monte Carlo Approach for Data Inversion of Observations of Titan's Seas." IEEE Trans. Geoscience and Remote Sensing 54.10 (2016): 5646-5656.

Mastrogiuseppe, Marco, et al. "The bathymetry of a Titan sea." Geophysical Research Letters 41.5 (2014): 1432-1437.

Mitchell, Karl L., et al. "Laboratory measurements of cryogenic liquid alkane microwave absorptivity and implications for the composition of Ligeia Mare, Titan." Geophysical Research Letters 42.5 (2015): 1340-1345.

Paillou, Philippe, et al. "Microwave dielectric constant of Titan-relevant materials." Geophysical Research Letters 35.18 (2008).

Stephan, Katrin, et al. "Specular reflection on Titan: liquids in Kraken Mare." Geophysical Research Letters 37.7 (2010).

Wye, L. C., H. A. Zebker, and R. D. Lorenz. "Smoothness of Titan's Ontario Lacus: Constraints from Cassini RADAR specular reflection data." Geophysical Research Letters 36.16 (2009).

Zebker, Howard, et al. "Surface of Ligeia Mare, Titan, from Cassini altimeter and radiometer analysis." Geophysical Research Letters 41.2 (2014): 308-313.